Basic Notions of the Non-Markovian Redfield Equation

Wenxiang Ying *

July 21, 2024

Contents

1 Theory **2**
1.1 Projection Operator Formalism . . . 2
1.1.1 Time-nonlocal version . . . 2
1.1.2 Time-local equivalence . . . 4
1.1.3 Comments on the time-nonlocal and time-local equations . . . 4
1.2 Second Order Quantum Master Equations . . . 5
1.2.1 Time-nonlocal equation . . . 5
1.2.2 Time-local equation . . . 5
1.2.3 Remarks on the 2nd order time-local and time-nonlocal equations . . . 6
1.3 Representation and Approximations . . . 6
1.3.1 Adiabatic representation . . . 6
1.3.2 Explicit results for the Caldeira-Leggett model . . . 7
1.3.3 Markovian approximation . . . 8
1.3.4 Secular approximation . . . 9
1.3.5 Remarks on numerical implementation, and properties . . . 11

2 Numerical Examples **13**
2.1 The Spin-Boson Model . . . 13
2.1.1 Ohmic spectral density . . . 13
2.1.2 Debye spectral density . . . 13
2.2 The Fenna-Matthews-Olson Pigment-Protein Complex . . . 14

*wying3@ur.rochester.edu

1 Theory

1.1 Projection Operator Formalism

For a given Hamiltonian expressed as

$$\hat{H}(t) = \hat{H}_0 + \hat{H}_1(t), \tag{1}$$

where $\hat{H}_0 = \hat{H}_{\rm S} + \hat{h}_{\rm B}$ and $\hat{H}_1(t)$ are the unperturbed part (which consists of the bare system Hamiltonian $\hat{H}_{\rm S}$ and the bare bath Hamiltonian $\hat{h}_{\rm B}$) and the perturbation, respectively. Under the $\hat{H}_0$-interaction picture, the Liouville-von Neumann equation for the total density matrix $\hat{\rho}_I(t)$ is

$$\frac{d}{dt}\hat{\rho}_I(t) = -i\mathcal{L}_I(t)\hat{\rho}_I(t), \tag{2}$$

where $\hat{\rho}_I(t) = \mathcal{G}_0^\dagger(t)\hat{\rho}(t)$, with $\hat{\rho}(t)$ the total density matrix under the Schrödinger picture, and $\mathcal{G}_0(t)$ the free superpropagator. Further, $\mathcal{L}_I(t)\cdot = [\hat{H}_1^I(t), \cdot]$ with $\hat{H}_1^I(t) = \hat{H}_1(t)\mathcal{G}_0^\dagger(t)$. Note that we have chosen $\hbar = 1$ throughout this Note for simplicity.

The system reduced density matrix (RDM) is defined as $\hat{\rho}_{\rm S}(t) := {\rm Tr}_{\rm B}[\hat{\rho}(t)]$, where ${\rm Tr}_{\rm B}[\cdot]$ takes the partial trace over the bath degrees of freedom (DOF). To obtain the dynamics of the RDM, we introduce a projection operator as follows,

$$\mathcal{P}\cdot := \hat{\rho}_{\rm B} \otimes {\rm Tr}_{\rm B}[\cdot], \qquad \mathcal{Q} := 1 - \mathcal{P}. \tag{3}$$

It is straightforward to see that $\mathcal{P}\mathcal{Q} = 0$. And the RDM under the interaction picture can also obtained via $\hat{\rho}_{\rm S}^I(t) = {\rm Tr}_{\rm B}[\mathcal{P}\hat{\rho}_I(t)]$.

With the above definitions, one obtains the following equations of motion,

$$\frac{d}{dt}\mathcal{P}\hat{\rho}_I(t) = -i\mathcal{P}\mathcal{L}_I(t)(\mathcal{P}+\mathcal{Q})\hat{\rho}_I(t), \tag{4}$$

$$\frac{d}{dt}\mathcal{Q}\hat{\rho}_I(t) = -i\mathcal{Q}\mathcal{L}_I(t)(\mathcal{P}+\mathcal{Q})\hat{\rho}_I(t). \tag{5}$$

1.1.1 Time-nonlocal version

Formal integration of Eq. 5 from zero time to t leads to

$$\mathcal{Q}\hat{\rho}_I(t) = -i\int_0^t d\tau\ \exp_+\Big[-i\int_\tau^t ds\ \mathcal{Q}\mathcal{L}_I(s)\Big]\mathcal{Q}\mathcal{L}_I(\tau)\mathcal{P}\hat{\rho}_I(\tau) + \exp_+\Big[-i\int_{t_0}^t d\tau\ \mathcal{Q}\mathcal{L}_I(\tau)\Big]\mathcal{Q}\hat{\rho}_I(0). \tag{6}$$

Plug Eq. 6 into Eq. 4, one obtains

$$\begin{aligned}\frac{d}{dt}\mathcal{P}\hat{\rho}_I(t) = &-i\mathcal{P}\mathcal{L}_I(t)\mathcal{P}\hat{\rho}_I(t) - \mathcal{P}\int_0^t d\tau\ \mathcal{L}_I(t)\exp_+\Big[-i\int_\tau^t ds\ \mathcal{Q}\mathcal{L}_I(s)\Big]\mathcal{Q}\mathcal{L}_I(\tau)\mathcal{P}\hat{\rho}_I(\tau)\\ &- i\mathcal{P}\mathcal{L}_I(t)\exp_+\Big[-i\int_{t_0}^t d\tau\ \mathcal{Q}\mathcal{L}_I(\tau)\Big]\mathcal{Q}\hat{\rho}_I(0),\end{aligned} \tag{7}$$

which can be re-expressed as

$$\begin{aligned}\hat{\rho}_{\rm B}^{\rm eq}\otimes\frac{d}{dt}\hat{\rho}_{\rm S}^{I}(t) = &-i\hat{\rho}_{\rm B}^{\rm eq}\otimes{\rm Tr}_{\rm B}\Big[\mathcal{L}_I(t)\hat{\rho}_{\rm B}^{\rm eq}\Big]\hat{\rho}_{\rm S}^{I}(t)\\ &-\hat{\rho}_{\rm B}^{\rm eq}\otimes{\rm Tr}_{\rm B}\left[\int_0^t d\tau\ \mathcal{L}_I(t)\exp_+\Big[-i\int_\tau^t ds\ \mathcal{Q}\mathcal{L}_I(s)\Big]\mathcal{Q}\mathcal{L}_I(\tau)\hat{\rho}_{\rm B}^{\rm eq}\right]\hat{\rho}_{\rm S}^{I}(\tau)\\ &-i\hat{\rho}_{\rm B}^{\rm eq}\otimes{\rm Tr}_{\rm B}\left[\mathcal{L}_I(t)\exp_+\Big[-i\int_{t_0}^t d\tau\ \mathcal{Q}\mathcal{L}_I(\tau)\Big]\mathcal{Q}\hat{\rho}_I(0)\right].\end{aligned}\tag{8}$$

Taking partial trace over the bath DOF for the above equation leads to

$$\frac{d}{dt}\hat{\rho}_{\rm S}^{I}(t) = -i{\rm Tr}_{\rm B}\Big[\mathcal{L}_I(t)\hat{\rho}_{\rm B}^{\rm eq}\Big]\hat{\rho}_{\rm S}^{I}(t) - \int_0^t d\tau\ \mathcal{K}(t-\tau)\hat{\rho}_{\rm S}^{I}(\tau) + \mathcal{I}(t,0),\tag{9}$$

where the memory kernel $\mathcal{K}(t-\tau)$ is defined as

$$\mathcal{K}(t-\tau) := {\rm Tr}_{\rm B}\left[\mathcal{L}_I(t)\exp_+\Big[-i\int_\tau^t ds\ \mathcal{Q}\mathcal{L}_I(s)\Big]\mathcal{Q}\mathcal{L}_I(\tau)\hat{\rho}_{\rm B}^{\rm eq}\right],\tag{10}$$

captures the effects of the bath on the system over the time interval from 0 to t, reflecting non-Markovian dynamics where the system's history influences its future evolution. Further, the inhomogeneous term $\mathcal{I}(t,0)$ is defined as

$$\mathcal{I}(t,0) := -i{\rm Tr}_{\rm B}\left[\mathcal{L}_I(t)\exp_+\Big[-i\int_{t_0}^t d\tau\ \mathcal{Q}\mathcal{L}_I(\tau)\Big]\mathcal{Q}\hat{\rho}_I(0)\right],\tag{11}$$

which characterizes the influence of the initial state of the bath on the system at time t, which is crucial for accurately describing the system dynamics from an initial condition.

Suppose the system is initialized from a product state, where there is no system-bath correlation at $t=0$ so that the total density matrix is separable, *i.e.*,

$$\hat{\rho}_I(0) = \hat{\rho}(0) = \hat{\rho}_{\rm S}(0)\otimes\hat{\rho}_{\rm B}^{\rm eq},\tag{12}$$

where $\hat{\rho}_{\rm B}^{\rm eq} = e^{-\beta\hat{h}_{\rm B}}/{\rm Tr}_{\rm B}[e^{-\beta\hat{h}_{\rm B}}]$, with $\beta = 1/(k_{\rm B}T)$. As such, $\mathcal{P}\hat{\rho}_I(0) = \hat{\rho}_I(0)$, which results in $\mathcal{Q}\mathcal{P}\hat{\rho}_I(0) = 0$, and the inhomogeneous term defined in Eq. 11 disappear. We further assume a *tricky* identity holds [see Chapter 5, Eq. (5.7) of Ref. [1]]:

$$\mathcal{P}\mathcal{L}_I(t)\mathcal{P} = 0,\tag{13}$$

which can always be satisfied by appropriate denition of $\hat{H}_1(t)$. As such, the first term in the right-hand side of Eq. 9 also disappear, which helps simplify the final expression of Eq. 9 as follows

$$\frac{d}{dt}\hat{\rho}_{\rm S}^{I}(t) = -\int_0^t d\tau\ \mathcal{K}(t-\tau)\hat{\rho}_{\rm S}^{I}(\tau).\tag{14}$$

Eq. 14 is featured in the form of time convolution of a memory kernel with the RDM at an earlier time, known as the *Nakajima-Zwanzig-Mori* formalism, which is formally exact.

1.1.2 Time-local equivalence

According to Shibata [2], one can alternatively recast the time convolution master equation into a time convolution less form. This is described as follows. According to Eq. 2, the total density matrix evolves backward in time as

$$\hat{\rho}_I(\tau) = \exp_-\Big[i\int_\tau^t ds\ \mathcal{L}_I(s)\Big]\hat{\rho}_I(t). \tag{15}$$

Replacing the $\hat{\rho}_I(\tau)$ in Eq. 6, and make use of Eq. 12 to get rid of the initial condition dependent term, one obtains

$$\mathcal{Q}\hat{\rho}_I(t) = \Sigma(t)(\mathcal{P}+\mathcal{Q})\hat{\rho}_I(t), \tag{16}$$

where for simplicity, we denote the superoperator

$$\Sigma(t) := -i\int_0^t d\tau\ \exp_+\Big[-i\int_\tau^t ds\ \mathcal{Q}\mathcal{L}_I(s)\Big]\mathcal{Q}\mathcal{L}_I(\tau)\mathcal{P}\exp_-\Big[i\int_\tau^t ds\ \mathcal{L}_I(s)\Big]. \tag{17}$$

From Eq. 16, one can separate the $\mathcal{Q}\hat{\rho}_I(t)$ term as follows,

$$\mathcal{Q}\hat{\rho}_I(t) = [1-\Sigma(t)]^{-1}\Sigma(t)\mathcal{P}\hat{\rho}_I(t). \tag{18}$$

Note that a crucial requirement for the validity of the above derivation is the existence of the inverse $[1-\Sigma(t)]^{-1}$. Plug Eq. 18 into Eq. 4 and subsequently take the partial trace for the bath DOF, one obtains a time-local equation of motion for the RDM as follows,

$$\frac{d}{dt}\hat{\rho}_{\mathrm{S}}^I(t) = \mathcal{R}(t)\hat{\rho}_{\mathrm{S}}^I(t), \tag{19}$$

where the (time local) rate function is expressed as

$$\mathcal{R}(t) := -i\mathrm{Tr}_{\mathrm{B}}\Big[\mathcal{L}_I(t)[1-\Sigma(t)]^{-1}\Sigma(t)\hat{\rho}_{\mathrm{B}}^{\mathrm{eq}}\Big]. \tag{20}$$

Eq. 19 is known as the *Tokuyama–Mori* formalism, which is also formally exact.

1.1.3 Comments on the time-nonlocal and time-local equations

Although both Eq. 14 and Eq. 19 are formally exact, the exact memory kernel $\mathcal{K}(t-\tau)$ (or the rate function $\mathcal{R}(t)$) is difficult to calculate except for several analytically solvable models. The exact calculation of the memory kernel or the rate function usually depends on the exact RDM obtained from other methods (HEOM, MCTDH, etc.), examples can be found in Ref. [3, 4].

The more useful ones involve approximations to different extents / schemes. For example, truncated generalized cumulant expansions. A large class of quantum master equations (QMEs) employ perturbative approximation for the term $\exp_+\Big[-i\int_\tau^t ds\ \mathcal{Q}\mathcal{L}_I(s)\Big]$ (either in Eq. 10 or Eq. 17) and come under different names depending on the choices of the parameter and representation of the Hamiltonian, the order of approximation, the choice of basis set, or sometimes the choice of numerical strategy, *etc.*

Within the Nakajima-Zwanzig framework, one can choose between (1) time convolution (TC) [or time-nonlocal (TNL) as interchangeable phrase], and (2) time convolution less (TCL) [or time-local (TL) as interchangeable phrase] forms of the QMEs. The TC approach involves memory effects, where the future state of the system depends on its entire history (Non-Markovian dynamics). The TCL approach formulates the dynamics where the system's rate of change at any moment depends only on its current state, simplifying calculations by neglecting memory effects (Markovian dynamics).

1.2 Second Order Quantum Master Equations

The simplest approximation from the exact formal exact equations are the 2nd order approximations. Let us consider a general form of system-bath coupling Hamiltonian,

$$\hat{H}_1(t) = \sum_a \hat{S}_a(t) \otimes \hat{F}_a(t), \tag{21}$$

where $\hat{S}_a(t)$ and $\hat{F}_a(t)$ are the a-th system and bath dissipation modes, respectively.

1.2.1 Time-nonlocal equation

The time-nonlocal equation can be established from Eq. 14, where the memory kernel defined in Eq. 10 is approximated as

$$\mathcal{K}(t-\tau) \approx \mathcal{K}^{(2)}(t-\tau) := \mathrm{Tr}_{\mathrm{B}}\Big[\mathcal{L}_I(t)\mathcal{L}_I(\tau)\hat{\rho}_{\mathrm{B}}^{\mathrm{eq}}\Big], \tag{22}$$

in which we kept terms only up to the 2nd order. The above approximation is known as the *Born approximation*. Under the interaction picture, the operators are transformed from Heisenberg picture via

$$\hat{H}_1^I(t) = \sum_a \hat{S}_a^I(t) \otimes \hat{F}_a^I(t), \tag{23}$$

where

$$\hat{S}_a^I(t) = \hat{S}_a(t)\mathcal{G}_0^\dagger(t), \qquad \hat{F}_a^I(t) = \hat{F}_a(t)\mathcal{G}_0^\dagger(t). \tag{24}$$

Inserting Eq. 23 into Eq. 22, one obtains

$$\mathcal{K}^{(2)}(t-\tau)\hat{\rho}_I(\tau) = \sum_{a,b} C_{ab}(t-\tau)\Big[\hat{S}_a^I(t), \hat{S}_b^I(\tau)\hat{\rho}_I(\tau)\Big] + \mathrm{h.c.}, \tag{25}$$

where h.c. represents Hermitian conjugate, and the bare-bath time-correlation functions (TCF) are defined as

$$C_{ab}(t-\tau) := \mathrm{Tr}_{\mathrm{B}}\Big[\hat{F}_a^I(t)\hat{F}_b^I(\tau)\hat{\rho}_{\mathrm{B}}^{\mathrm{eq}}\Big]. \tag{26}$$

As a result, the 2nd order time-nonlocal master equation uses Eq. 25 in Eq. 14.

1.2.2 Time-local equation

Similarly, the time-local equation can be established from Eq. 19, where the rate function defined in Eq. 20 is approximated as

$$\mathcal{R}(t) \approx \mathcal{R}^{(2)}(t) = \int_0^t d\tau\ \mathrm{Tr}_{\mathrm{B}}\Big[\mathcal{L}_I(t)\mathcal{L}_I(\tau)\hat{\rho}_{\mathrm{B}}^{\mathrm{eq}}\Big]. \tag{27}$$

As a result,

$$\mathcal{R}^{(2)}(t)\hat{\rho}_{\mathrm{S}}^I(t) = \sum_{a,b}\int_0^t d\tau\ C_{ab}(t-\tau)\Big[\hat{S}_a^I(t), \hat{S}_b^I(\tau)\hat{\rho}_{\mathrm{S}}^I(t)\Big] + \mathrm{h.c.}, \tag{28}$$

or equivalently, by changing integration variable $\tau \to t - \tau$,

$$\mathcal{R}^{(2)}(t)\hat{\rho}_{\rm S}^I(t) = \sum_{a,b} \int_0^t d\tau\ C_{ab}(\tau)\Big[\hat{S}_a^I(t), \hat{S}_b^I(t-\tau)\hat{\rho}_{\rm S}^I(t)\Big] + \text{h.c.}. \tag{29}$$

The 2nd order time-local master equation uses Eq. 29 in Eq. 19, which is a non-Markovian generalization of the Redfield theory (as the original Bloch-Redfield theory is formulated in a Markovian form [5, 6, 7]), known as the *non-Markovian Redfield equation*. Under the Schrödinger picture, it reads as

$$\begin{aligned}\frac{d}{dt}\hat{\rho}_{\rm S}(t) = -i[\hat{H}_{\rm S}, \hat{\rho}_{\rm S}(t)] - \sum_{a,b}\int_0^t d\tau\ \Big\{ & C_{ab}(\tau)\Big[\hat{S}_a, \hat{S}_b(-\tau)\hat{\rho}_{\rm S}(t)\Big] \\ & - C_{ba}(-\tau)\Big[\hat{S}_a, \hat{\rho}_{\rm S}(t)\hat{S}_b(-\tau)\Big]\Big\},\end{aligned} \tag{30}$$

where $\hat{S}_b(-\tau) = e^{-i\hat{H}_{\rm S}\tau}\hat{S}_b e^{i\hat{H}_{\rm S}\tau}$.

1.2.3 Remarks on the 2nd order time-local and time-nonlocal equations

The 2nd order time-local master equation (TL-2) and time-nonlocal master equation (TNL-2) have similar formalism, where the only difference is that TL-2 replaces $\hat{\rho}_I(\tau)$ in TNL-2 as $\hat{\rho}_I(t)$. It is thus usually believed that TL-2 is less accurate than TNL-2. However, this is not true in general because the influence of the higher order terms are uncontrolled. There are counter examples suggesting that TL-2 performs better than TNL-2, depending on the details of the bath Hamiltonian as well as their coupling to the system [1].

1.3 Representation and Approximations

We further discuss the representation and approximations based on the TL-2 equation, as well as the numerical implementation tricks.

1.3.1 Adiabatic representation

Practically, one will choose a basis to represent the system Hamiltonian $\hat{H}_{\rm S}$ as well as the RDM. The adiabaic basis (eigen basis of $\hat{H}_{\rm S}$) is the most convenient one to implement TL-2. Define the eigen basis set of $\hat{H}_{\rm S}$ as $\{|\mu\rangle\}$, whose eigen energies are $\hat{H}_{\rm S}|\mu\rangle = \epsilon_\mu|\mu\rangle$. Further denote the transition frequencies between two adiabatic states $|\mu\rangle$ and $|\nu\rangle$ as

$$\omega_{\mu\nu} := \epsilon_\mu - \epsilon_\nu.$$

The matrix elements for the RDO and system operators are expressed as

$$[\rho_{\rm S}]_{\mu\nu}(t) := \langle\mu|\hat{\rho}_{\rm S}(t)|\nu\rangle, \quad [S_a]_{\mu\nu} := \langle\mu|\hat{S}_a|\nu\rangle. \tag{31}$$

As such, TL-2 is expressed under the Schrödinger picture as

$$\frac{d}{dt}[\rho_{\rm S}]_{\mu\nu}(t) = -i\omega_{\mu\nu}[\rho_{\rm S}]_{\mu\nu}(t) + \sum_{\mu'\nu'}\mathcal{R}_{\mu\nu\mu'\nu'}(t)[\rho_{\rm S}]_{\mu'\nu'}(t), \tag{32}$$

where the Redfield tensor $\mathcal{R}_{\mu\nu\mu'\nu'}(t)$ is defined as follows,

$$\mathcal{R}_{\mu\nu\mu'\nu'}(t) := \Gamma^{>}_{\nu'\nu\mu\mu'}(t) + \Gamma^{<}_{\nu'\nu\mu\mu'}(t) - \delta_{\nu\nu'}\sum_{\kappa}\Gamma^{>}_{\mu\kappa\kappa\mu'}(t) - \delta_{\mu\mu'}\sum_{\kappa}\Gamma^{<}_{\nu'\kappa\kappa\nu}(t), \tag{33}$$

and

$$\Gamma^{>}_{\mu\nu\mu'\nu'}(t) := \sum_{a,b}\int_0^t d\tau\ C_{ab}(\tau)e^{-i\omega_{\mu'\nu'}\tau}[S_a]_{\mu\nu}[S_b]_{\mu'\nu'}, \tag{34}$$

$$\Gamma^{<}_{\mu\nu\mu'\nu'}(t) := \sum_{a,b}\int_0^t d\tau\ C_{ba}(-\tau)e^{-i\omega_{\mu\nu}\tau}[S_b]_{\mu\nu}[S_a]_{\mu'\nu'}. \tag{35}$$

When the bath operators are Hermitian, one has $C_{ba}(-\tau) = C^*_{ab}(\tau)$ due to the time-reversal symmetry. As a result, $\Gamma^{<}_{\nu'\nu\mu\mu'}(t) = [\Gamma^{>}_{\mu'\mu\nu\nu'}(t)]^*$, and Eq. 33 is simplified as

$$\mathcal{R}_{\mu\nu\mu'\nu'}(t) = \Gamma_{\nu'\nu\mu\mu'}(t) + \Gamma^*_{\mu'\mu\nu\nu'}(t) - \delta_{\nu\nu'}\sum_{\kappa}\Gamma_{\mu\kappa\kappa\mu'}(t) - \delta_{\mu\mu'}\sum_{\kappa}\Gamma^*_{\nu\kappa\kappa\nu'}(t), \tag{36}$$

where we denote $\Gamma_{\nu'\nu\mu\mu'}(t) := \Gamma^{>}_{\nu'\nu\mu\mu'}(t)$ for simplicity.

1.3.2 Explicit results for the Caldeira-Leggett model

Further, the time-dependent component in $\Gamma_{\nu'\nu\mu\mu'}(t)$ is expressed as

$$\tilde{C}_{\mu'\nu'}(t) := \sum_{a,b}\int_0^t d\tau\ C_{ab}(\tau)e^{-i\omega_{\mu'\nu'}\tau}. \tag{37}$$

For the commonly used Caldeira-Leggett model [8], where the bath consists of a set of non-interacting harmonic oscillators that are linearly coupled to the system, *i.e.*,

$$\hat{h}_{\mathrm{B}} = \frac{1}{2}\sum_j \omega_j(\hat{x}_j^2 + \hat{p}_j^2), \qquad \hat{F}_a := \sum_j c_{aj}\hat{x}_j. \tag{38}$$

One thus has the bosonic fluctuation-dissipation theorem (FDT) as follows,

$$C_{ab}(t) = \frac{1}{\pi}\int_{-\infty}^{+\infty} d\omega\ \frac{\mathcal{J}_{ab}(\omega)e^{-i\omega t}}{1-e^{-\beta\omega}} = \frac{1}{2\pi}\int_{-\infty}^{+\infty} d\omega\ \mathcal{J}_{ab}(\omega)\left[\coth\left(\frac{\beta\omega}{2}\right)\cos(\omega t) - i\sin(\omega t)\right], \tag{39}$$

where for the second equal sign, we have used the following identity,

$$\frac{1}{1-e^{-\beta\omega}} = \frac{1}{2}\left[1 + \coth\left(\frac{\beta\omega}{2}\right)\right]. \tag{40}$$

Using the bosonic FDT in Eq. 39, Eq. 37 becomes

$$\tilde{C}_{\mu'\nu'}(t) = \int_0^t d\tau\ e^{-i\omega_{\mu'\nu'}\tau} \times \frac{1}{2\pi}\sum_{a,b}\int_{-\infty}^{+\infty} d\omega\ \mathcal{J}_{ab}(\omega)\left[\coth\left(\frac{\beta\omega}{2}\right)\cos(\omega\tau) - i\sin(\omega\tau)\right], \tag{41}$$

where $\mathcal{J}_{ab}(\omega)$ are the bath spectral density functions, expressed as follows,

$$\mathcal{J}_{ab}(\omega) := \frac{1}{2}\int_{-\infty}^{+\infty} dt\ e^{i\omega t}\langle[\hat{F}_a(t), \hat{F}_b(0)]\rangle_{\mathrm{B}} = \frac{\pi}{2}\sum_j \frac{c_{aj}c_{bj}}{\omega_j}[\delta(\omega-\omega_j) - \delta(\omega+\omega_j)]. \tag{42}$$

Note that the spectral density function $\mathcal{J}_{ab}(\omega)$ has been extended to negative frequencies via analytical continuation, $\mathcal{J}_{ab}(\omega) = -\mathcal{J}_{ab}(-\omega)$, being an odd function. Using the discretized form of the spectral density in Eq. 42, Eq. 41 can be further expressed analytically as follows,

$$\begin{aligned}
\tilde{C}_{\mu'\nu'}(t) &= \sum_{a,b,j}\frac{c_{aj}c_{bj}}{2\omega_j}\int_0^t d\tau\ \left[\coth\left(\frac{\beta\omega_j}{2}\right)\cos(\omega_j\tau) - i\sin(\omega_j\tau)\right]e^{i\omega_{\nu'\mu'}\tau} \\
&= \sum_{a,b,j}\frac{c_{aj}c_{bj}}{2\omega_j}\int_0^t d\tau\ \left[\coth\left(\frac{\beta\omega_j}{2}\right)\frac{e^{i\omega_j\tau}+e^{-i\omega_j\tau}}{2} - i\frac{e^{i\omega_j\tau}-e^{-i\omega_j\tau}}{2i}\right]e^{i\omega_{\nu'\mu'}\tau} \\
&= \sum_{a,b,j}\frac{c_{aj}c_{bj}}{2\omega_j}\int_0^t d\tau\ \left[\frac{\coth(\beta\omega_j/2)-1}{2}e^{i(\omega_j+\omega_{\nu'\mu'})\tau} + \frac{\coth(\beta\omega_j/2)+1}{2}e^{i(\omega_{\nu'\mu'}-\omega_j)\tau}\right] \\
&= \sum_{a,b,j}\frac{c_{aj}c_{bj}}{2\omega_j}\left[n_{\mathrm{BE}}(\omega_j)\frac{e^{i(\omega_{\mu'\nu'}+\omega_j)t}-1}{i(\omega_{\mu'\nu'}+\omega_j)} + [n_{\mathrm{BE}}(\omega_j)+1]\frac{e^{i(\omega_{\nu'\mu'}-\omega_j)t}-1}{i(\omega_{\nu'\mu'}-\omega_j)}\right] \\
&= i\sum_{a,b,j}\frac{c_{aj}c_{bj}}{2\omega_j}\left[[n_{\mathrm{BE}}(\omega_j)+1]\frac{1-e^{i(\omega_{\mu'\nu'}-\omega_j)t}}{\omega_{\mu'\nu'}-\omega_j} + n_{\mathrm{BE}}(\omega_j)\frac{1-e^{i(\omega_{\mu'\nu'}+\omega_j)t}}{\omega_{\mu'\nu'}+\omega_j}\right],
\end{aligned} \tag{43}$$

where

$$n_{\mathrm{BE}}(\omega) = 1/(e^{\beta\omega}-1) \tag{44}$$

is the Bose-Einstein distribution function. Then

$$\Gamma_{\mu\nu\mu'\nu'}(t) = \sum_{ab}\tilde{C}_{\mu'\nu'}(t)[S_a]_{\mu\nu}[S_b]_{\mu'\nu'}, \tag{45}$$

which has an analytic closed form expression and can be numerically implemented directly to build the time-dependent Redfield tensor in Eq. 36.

1.3.3 Markovian approximation

Similar to the Pauli master equation, it is assumed that the relaxation tensor changes slowly in time, and it can be assumed constant for the duration of the interaction described by the interaction Hamiltonian. Under the long time limit, the time-dependent Redfield tensor can be approximated as time-independent. Extend the upper limit of the integral to infinity, $\int_0^t d\tau \ \rightarrow \int_0^\infty d\tau$ in the master equation, which is known as the *Markovian approximation*, and Eq. 30 becomes

$$\begin{aligned}
\frac{d}{dt}\hat{\rho}_{\mathrm{S}}(t) = -i[\hat{H}_{\mathrm{S}}, \hat{\rho}_{\mathrm{S}}(t)] - \sum_{a,b}\int_0^\infty d\tau\ \Big\{&C_{ab}(\tau)\Big[\hat{S}_a, \hat{S}_b(-\tau)\hat{\rho}_{\mathrm{S}}(t)\Big] \\
&- C_{ba}(-\tau)\Big[\hat{S}_a, \hat{\rho}_{\mathrm{S}}(t)\hat{S}_b(-\tau)\Big]\Big\},
\end{aligned} \tag{46}$$

which is the Markovian Redfield equation. As a result, one can extract the time-dependent part and define the dressed system operators as follows,

$$\hat{\tilde{S}}_a := \sum_b \int_0^\infty d\tau\ C_{ab}(\tau)\hat{S}_b(-\tau) = \sum_b C_{ab}(-\mathcal{L}_{\rm S})\hat{S}_b, \tag{47}$$

where the *bath correlation spectrum function* is defined via the causality Fourier transform of the bath TCFs as follows,

$$C_{ab}(\omega) := \int_0^\infty dt\ e^{i\omega t}\langle \hat{F}_a(t)\hat{F}_b(0)\rangle_{\rm B}. \tag{48}$$

Then Eq. 46 can be alternatively expressed as

$$\frac{d}{dt}\hat{\rho}_{\rm S}(t) = -i[\hat{H}_{\rm S}, \hat{\rho}_{\rm S}(t)] - \sum_a \Big[\hat{S}_a, \hat{\tilde{S}}_a\hat{\rho}_{\rm S}(t) - \hat{\rho}_{\rm S}(t)\hat{\tilde{S}}_a^\dagger\Big]. \tag{49}$$

Equivalently, the time-dependent Redfield tensors under the adiabatic representation also become time-independent, reading as (c.f. Eq. 33-34)

$$\Gamma^{>}_{\mu\nu\mu'\nu'}(t) \to \Gamma^{>}_{\mu\nu\mu'\nu'}(\omega_{\nu'\mu'}) := \sum_{a,b}\int_0^\infty d\tau\ C_{ab}(\tau)e^{-i\omega_{\mu'\nu'}\tau}[S_a]_{\mu\nu}[S_b]_{\mu'\nu'} = \sum_{a,b} C_{ab}(\omega_{\nu'\mu'})[S_a]_{\mu\nu}[S_b]_{\mu'\nu'}, \tag{50}$$

where the correlation spectrum functions $C_{ab}(\omega)$ are defined in Eq. 48. If the bath operators are Hermitian, so that there will be time reversal symmetry for the bare-bath TCFs, *i.e.*, $C_{ab}(t) = C^*_{ba}(-t)$, then $\Gamma^{<}_{\mu\nu\mu'\nu'} = [\Gamma^{>}_{\nu'\mu'\mu\nu}]^*$. As a result, the time-independent Redfield tensor reads as (c.f. Eq. 33)

$$\mathcal{R}_{\mu\nu\mu'\nu'} = \Gamma_{\nu'\nu\mu\mu'}(\omega_{\mu'\mu}) + \Gamma^*_{\mu'\mu\nu\nu'}(\omega_{\nu'\nu}) - \delta_{\nu\nu'}\sum_\kappa \Gamma_{\mu\kappa\kappa\mu'}(\omega_{\mu'\kappa}) - \delta_{\mu\mu'}\sum_\kappa \Gamma^*_{\nu\kappa\kappa\nu'}(\omega_{\nu'\kappa}). \tag{51}$$

1.3.4 Secular approximation

The secular approximation involves discarding fast oscillating terms (without frequency matching) in the Markovian master equation. It is therefore similar to the rotating-wave approximation (RWA) used in NMR and quantum optics, which comes from the fact that optical transition frequencies are much larger than the decay rates of excited states. However, applying the RWA directly on the level on the interaction Hamiltonian can cause problems such as an incorrect renormalization of the system Hamiltonian. The secular approximation, on the other hand, is carried out on the level of the quantum master equation, which leads to the outcome that the population and coherence of the RDM evolves independently, and gives rise to the structure of Lindbladian.

To be specific, first, we explicitly write down the Markovian Redfield equation in terms of matrix elements using Eq. 51,

$$\begin{aligned}\frac{d}{dt}\rho_{\mu\nu}(t) = &-i\omega_{\mu\nu}\rho_{\mu\nu}(t) + \sum_{\mu'\nu'}[\Gamma_{\nu'\nu\mu\mu'}(\omega_{\mu'\mu}) + \Gamma^*_{\mu'\mu\nu\nu'}(\omega_{\nu'\nu})]\rho_{\mu'\nu'}(t)\\ &- \sum_{\mu'\nu'}[\Gamma_{\mu\nu'\nu'\mu'}(\omega_{\mu'\nu'})\rho_{\mu'\nu}(t) + \Gamma^*_{\nu\mu'\mu'\nu'}(\omega_{\nu'\mu'})\rho_{\mu\nu'}(t)].\end{aligned} \tag{52}$$

Let us consider the case of population evolution when $\mu = \nu$ (diagonal matrix elements only), which leads to

$$\frac{d}{dt}\rho_{\mu\mu}(t) = \sum_{\mu'}[\Gamma_{\mu'\mu\mu\mu'}(\omega_{\mu'\mu}) + \Gamma^*_{\mu'\mu\mu\mu'}(\omega_{\mu'\mu})]\rho_{\mu'\mu'}(t) - \sum_{\mu'}[\Gamma_{\mu\mu'\mu'\mu}(\omega_{\mu'\mu}) + \Gamma^*_{\mu\mu'\mu'\mu}(\omega_{\mu\mu'})]\rho_{\mu\mu}(t). \tag{53}$$

where in Eq. 52, among the four relaxation terms, we have taken $\nu' = \mu'$ for the first two terms, $\mu' = \mu$ for the third term then replace the summation for ν' to μ', and $\nu' = \mu$ for the fourth term. Eq. 53 is just the Pauli master equation for poulation relaxation,

$$\frac{d}{dt}P_\mu(t) = \sum_{\mu'} k_{\mu'\to\mu}P_{\mu'}(t) - \sum_{\mu'} k_{\mu\to\mu'}P_\mu(t), \tag{54}$$

where we have defined the population $P_\mu(t) := \rho_{\mu\mu}(t)$, and the transition rates

$$\begin{aligned} k_{\mu'\to\mu} &:= 2\mathrm{Re}\big[\Gamma_{\mu'\mu\mu\mu'}(\omega_{\mu'\mu})\big] = 2\sum_{a,b}\mathrm{Re}[C_{ab}(\omega_{\mu'\mu})][S_a]_{\mu'\mu}[S_b]_{\mu\mu'} \\ &= 2\sum_{a,b} J_{ab}(\omega_{\mu'\mu})[n_{\mathrm{BE}}(\omega_{\mu'\mu}) + 1][S_a]_{\mu'\mu}[S_b]_{\mu\mu'}, \end{aligned} \tag{55}$$

$$\begin{aligned} k_{\mu\to\mu'} &:= 2\mathrm{Re}\big[\Gamma_{\mu\mu'\mu'\mu}(\omega_{\mu'\mu})\big] = 2\sum_{a,b}\mathrm{Re}[C_{ab}(\omega_{\mu\mu'})][S_a]_{\mu\mu'}[S_b]_{\mu'\mu} \\ &= 2\sum_{a,b} J_{ab}(\omega_{\mu\mu'})[n_{\mathrm{BE}}(\omega_{\mu\mu'}) + 1][S_a]_{\mu\mu'}[S_b]_{\mu'\mu}. \end{aligned} \tag{56}$$

And the ratio between them

$$\begin{aligned} \frac{k_{\mu'\to\mu}}{k_{\mu\to\mu'}} &= \frac{2\sum_{a,b} J_{ab}(\omega_{\mu'\mu})[n_{\mathrm{BE}}(\omega_{\mu'\mu}) + 1][S_a]_{\mu'\mu}[S_b]_{\mu\mu'}}{2\sum_{a,b} J_{ab}(\omega_{\mu\mu'})[n_{\mathrm{BE}}(\omega_{\mu\mu'}) + 1][S_a]_{\mu\mu'}[S_b]_{\mu'\mu}} \\ &= -\frac{1/(e^{\beta\omega_{\mu'\mu}} - 1) + 1}{1/(e^{-\beta\omega_{\mu'\mu}} - 1) + 1} = \frac{e^{\beta\omega_{\mu'\mu}}}{e^{\beta\omega_{\mu'\mu}} - 1} \times (e^{\beta\omega_{\mu'\mu}} - 1) = e^{\beta\omega_{\mu'\mu}}, \end{aligned} \tag{57}$$

which is known as the *detailed balance relation.*

Next, let us consider the case of coherence evolution (off-diagonal elements) when $\mu \neq \nu$, which leads to

$$\frac{d}{dt}\rho_{\mu\nu}(t) = -i\omega_{\mu\nu}\rho_{\mu\nu}(t) - \sum_{\mu'}[\Gamma_{\mu\mu'\mu'\mu}(\omega_{\mu\mu'}) + \Gamma^*_{\nu\mu'\mu'\nu}(\omega_{\nu\mu'})]\rho_{\mu\nu}(t) + [\Gamma_{\nu\nu\mu\mu}(0) + \Gamma^*_{\mu\mu\nu\nu}(0) - \Gamma_{\mu\mu\mu\mu}(0) - \Gamma^*_{\nu\nu\nu\nu}(0)]\rho_{\mu\nu}(t), \tag{58}$$

where for the first two terms in the second line we have taken $\mu' = \mu$ and $\nu' = \nu$, while for the last two terms in the second line we have taken $\nu' = \mu$ and $\mu' = \nu$, respectively. By separating the real and imaginary parts of the Redfield tensors, Eq. 58 can be expressed as

$$\frac{d}{dt}\rho_{\mu\nu}(t) = -i\tilde{\omega}_{\mu\nu}\rho_{\mu\nu}(t) - \frac{1}{2}\Big[\sum_{\mu'\neq\mu} k_{\mu\to\mu'} + \sum_{\mu'\neq\nu} k_{\nu\to\mu'}\Big]\rho_{\mu\nu}(t) - \gamma_{\mu\nu}\rho_{\mu\nu}(t), \tag{59}$$

where the renormalized frequency

$$\tilde{\omega}_{\mu\nu} = \omega_{\mu\nu} + \sum_{\mu'\neq\mu} \mathrm{Im}\big[\Gamma_{\mu\mu'\mu'\mu}(\omega_{\mu\mu'})\big] + \sum_{\mu'\neq\nu} \mathrm{Im}\big[\Gamma^*_{\nu\mu'\mu'\nu}(\omega_{\nu\mu'})\big], \tag{60}$$

and the modification is known as the Lamb shift (which does not arise from RWA). Further, the population transfer rates are defined in Eq. 55, and

$$\begin{aligned}\gamma_{\mu\nu} &:= -[\Gamma_{\nu\nu\mu\mu}(0) + \Gamma^*_{\mu\mu\nu\nu}(0) - \Gamma_{\mu\mu\mu\mu}(0) - \Gamma^*_{\nu\nu\nu\nu}(0)] \\ &= ([S_a]_{\mu\mu} - [S_a]_{\nu\nu})([S_b]_{\mu\mu} - [S_b]_{\nu\nu}) \int_0^\infty d\tau\ C_{ab}(\tau).\end{aligned} \tag{61}$$

One can see from Eq. 59 that there are two processes that act to decay coherence. The first represents decoherence due to population transfer, which is usually referred to as the T_1 time, defined as $T_1^{-1} = \frac{1}{2}\Big[\sum_{\mu'\neq\mu} k_{\mu\to\mu'} + \sum_{\mu'\neq\nu} k_{\nu\to\mu'}\Big]$. And the second term represents pure dephasing (decoherence due to fluctuations in the energy gap $\omega_{\mu\nu}$ resulting from the coupling to the bath), which is usually referred to as the T_2 time, defined as $T_2^{-1} = \gamma_{\mu\nu}$.

Eq. 53 and Eq. 58 combines as the secular-approximated Redfield equation, where the population and coherence of the RDM evolves independently. In other words, there is no interdependence between the population and coherence, for instance, the time evolution of $\rho_{\mu\mu}(t)$ does not depend on the non-diagonal elements $\rho_{\mu\nu}(t)$. One can further obtain the Lindbladian after making the secular approximation, details can be found in Ref. [9].

1.3.5 Remarks on numerical implementation, and properties

1, RDM elements dynamics. For the non-Markovian Redfield equation expressed in terms of the RDM elements $[\rho_{\mathrm{S}}]_{\mu\nu}(t)$ (see Eq. 32), one can take advantage of the analytic closed form expression of the Redfield tensor in Eq. 45, which can be directly implemented in coding. Note that for finite number of bath oscillators $j = 1, \cdots, N_b$, the dynamics is, in principle, non-dissipative, one needs to take care of the Poincaré recurrence especially for long time propagation. Usually N_b should be large enough to converge the dynamics within given propagation length. To overcome the non-dissipative problem, one can alternatively discretize the time integral in Eq. 41, *i.e.*,

$$\tilde{C}_{\mu'\nu'}(t = t_N) = \Delta t \sum_{n=0}^{N} e^{-i\omega_{\mu'\nu't_n}} \times \frac{1}{\pi} \sum_{a,b} \int_{-\infty}^{\infty} d\omega\ \frac{\mathcal{J}_{ab}(\omega) e^{-i\omega t_n}}{1 - e^{-\beta\omega}}, \tag{62}$$

where Δt is the time step of the bath (which should be much smaller than the characteristic time scale of the bath), $t_n = n \cdot \Delta t$ for $n \in \{0, \cdots, N\}$ is the time corresponding to the n-th step of the dynamics. One needs to evaluate

$$\Delta t \cdot e^{-i\omega_{\mu'\nu't_n}} \times \sum_{a,b} C_{ab}(t) \tag{63}$$

for each time step t_n and add them up step by step (or performing numerical integration for the time interval Δt to stay more accurate). Note that one can still apply the discrete form spectral density function for Eq. 63 to proceed. The discretized time scheme is also very useful when the time integral with respect to TCFs cannot be evaluated analytically. For example, under the polaron transformed representation.

2, Matrix form. Nevertheless, under the RDM elements representation, if one applies 4-fold cycles to construct the Redfield tensor and calculate tensor-matrix products, then the algorithm complexity for the non-Markovian Redfield equation is at least $\mathcal{O}(N^4)$ where N is the dimension of the reduced system, which is very expensive to implement as it does not take advantage of any linear algebra modules that can potentially accelerate the calculations.

In contrast, the matrix form in Eq. 30 is more convenient for numerical implementation. For example, a much more efficient way is to use `np.kron` to construct the Redfield tensor, and use `np.einsum` to calculate tensor-matrix product, and update the Redfield tensor on-the-fly. We also recommend the readers to take a look at Ref. [10] and its Supplemental Material, which contains a lot of useful numerical tricks.

3, Properties of the Redfield equation. Redfield equations are trace-preserving and correctly produce a thermalized state for asymptotic propagation. However, in contrast to Lindblad equations, Redfield equations do not guarantee a positive time evolution of the density matrix. That is, it is possible to get negative populations during the time evolution. The Redfield equation approaches the correct dynamics for sufficiently weak coupling to the environment.

The 2nd order perturbative master equations are widely used due to their simplicity, while their validity can quickly degrade as the system-bath interaction becomes stronger (as they can only account for single phonon processes). Reichman, *et al.* [11] had provided an estimator that characterizes the accuracy of Redfield theory,

$$\eta = \max[2\lambda/(\beta\omega_{\mathrm{c}}^2), 2\lambda/(\pi\omega_{\mathrm{c}})], \tag{64}$$

where λ is the reorganization energy, ω_{c} is the bath characteristic frequency. Redfield theory becomes unreliable when $\eta > 1$.

2 Numerical Examples

In this section, we provide a bunch of numerical results of the non-Markovian Redfield equation for several typical model systems. The code implemented in these numerical calculations are available at `https://github.com/Okita0512/Non-Markovian-Redfield`.

2.1 The Spin-Boson Model

The spin-boson model Hamiltonian reads as follows,

$$\hat{H} = \epsilon\hat{\sigma}_z + \Delta\hat{\sigma}_x + \frac{1}{2}\sum_j \omega_j(\hat{x}_j^2 + \hat{p}_j^2) + \hat{\sigma}_z \otimes \hat{F}, \qquad \hat{F} \equiv \sum_j c_j\hat{x}_j. \tag{65}$$

According to the Caldeira-Leggett model, the bath as well as its interacting with the system can be described by the spectral density function, defined as follows,

$$J(\omega) \equiv \frac{1}{2}\int_{-\infty}^{+\infty} dt\ e^{i\omega t}\langle[\hat{F}(t), \hat{F}(0)]\rangle_{\mathrm{B}} = \frac{\pi}{2}\sum_{j=1}^{N}\frac{c_j^2}{\omega_j}\delta(\omega - \omega_j). \tag{66}$$

The reduced system is initially prepared on the excited state, *i.e.*, $\hat{\rho}_{\mathrm{S}}(0) = |e\rangle\langle e|$, and the bath is initially a thermal equilibrium state and decoupled from the system DOF, see Eq. 12.

2.1.1 Ohmic spectral density

The commonly used spectral density function is of the Ohmic form with exponential cutoff,

$$J(\omega) = \frac{\pi}{2}\alpha\omega e^{-\omega/\omega_{\mathrm{c}}}, \tag{67}$$

where α is the Kondo parameter, and ω_{c} is the bath characteristic frequency. The bare-bath TCF needs to be properly discretized. Here we adopt the following strategy,

$$\omega_j = -\omega_{\mathrm{c}}\ln[1 - j/(1 + N_b)], \qquad j = 1, \cdots, N_b, \tag{68a}$$

$$c_j = \sqrt{\frac{\alpha\omega_{\mathrm{c}}}{N_b + 1}}\omega_j, \qquad j = 1, \cdots, N_b, \tag{68b}$$

and N_b is the number of bath oscillators. A bunch of numerical examples are provided in Figure 1, and the validity of the Redfield theory can be evaluated using Eq. 64.

2.1.2 Debye spectral density

Another type of cutoff function for the Ohmic spectral density is the Lorentzian cutoff, known as the Debye spectral density or the Drude-Lorentz model, which is the overdamped limit of the Brownian oscillator. The Debye spectral density reads as follows,

$$J(\omega) = \frac{2\lambda\omega_{\mathrm{c}}\omega}{\omega^2 + \omega_{\mathrm{c}}^2}, \tag{69}$$

where λ is the reorganization energy, and ω_c is the bath characteristic frequency. One commonly used type of bath discretization procedure is described as follows,

$$\omega_j = \omega_c \tan\left[\frac{\pi}{2}\left(1 - \frac{j}{N_b+1}\right)\right], \qquad j = 1, \cdots, N_b, \tag{70a}$$

$$c_j = \sqrt{\frac{2\lambda}{N_b+1}}\omega_j, \qquad j = 1, \cdots, N_b, \tag{70b}$$

and N_b is the number of bath oscillators. A bunch of numerical examples are provided in Figure 2, and the validity of the Redfield theory can be evaluated using Eq. 64.

We also want to note that the discretization scheme for the Drude-Lorentz bath might be problematic for the implementation of the Redfield equation, due to the ill behavior of the TCF around $t \to 0$ (which is logarithmic divergent). As a result, the calculated population and coherence (especially for coherence) might face numerical issues.

2.2 The Fenna-Matthews-Olson Pigment-Protein Complex

The Fenna-Matthews-Olson (FMO) pigment-protein complex of green-sulfur bacteria acts as a mediator of excitation energy between the outer antenna system, i.e., the chlorosomes, and the reaction center [12, 13], transporting sunlight energy harvested in the chlorosome to the reaction center pigments.

The total Hamiltonian of the seven sites FMO model can be expressed in the system-bath form as follows,

$$\hat{H} = \hat{H}_S + \hat{h}_B + \hat{H}_{SB}, \tag{71}$$

where the system Hamiltonian is expressed as follows (with unit of cm^{-1}),

$$\hat{H}_S = \begin{bmatrix} 12410.0 & -87.7 & 5.5 & -5.9 & 6.7 & -13.7 & -9.9 \\ -87.7 & 12530.0 & 30.8 & 8.2 & 0.7 & 11.8 & 4.3 \\ 5.5 & 30.8 & 12210.0 & -53.5 & -2.2 & -9.6 & 6.0 \\ -5.9 & 8.2 & -53.5 & 12320.0 & -70.7 & -17.0 & -63.3 \\ 6.7 & 0.7 & -2.2 & -70.7 & 12480.0 & 81.1 & -1.3 \\ -13.7 & 11.8 & -9.6 & -17.0 & 81.1 & 12630.0 & 39.7 \\ -9.9 & 4.3 & 6.0 & -63.3 & -1.3 & 39.7 & 12440.0 \end{bmatrix}, \tag{72}$$

and the bath and system-bath coupling terms are

$$\hat{h}_B = \sum_{j=1}^{N=7} \sum_{\alpha} \frac{\omega_\alpha^2}{2}(\hat{p}_{j,\alpha}^2 + \hat{x}_{j,\alpha}^2), \tag{73}$$

$$\hat{H}_{SB} = -\sum_{j=1}^{N=7} |j\rangle\langle j| \otimes \hat{F}_j, \qquad \hat{F}_j := \sum_{\alpha} c_j \hat{x}_{j,\alpha}. \tag{74}$$

The baths as well as the system-bath couplings are described by Drude-Lorentz spectral density in Eq. 69, with discretization scheme introduced in Eq. 70a. The reorganization energy $\lambda = 35\ \mathrm{cm}^{-1}$, and characteristic frequency $\omega_c = 106.14\ \mathrm{cm}^{-1}$ (or a relaxation time of $\tau_c = 50$ fs, with $\omega_c = \tau_c^{-1}$), being identical for all the sites. The reduced system is initialized on the first site. Here we

consider two different temperatures, including the high temperature case with $T = 300$ K, and the low temperature case with $T = 77$ K. The numerical results are presented in Figure 3, which are compared with the numerically exact HEOM results [14, 15]. Note that for the 77 K case under the long time limit (10 ps), the Redfield results exhibit negative population. Interestingly, the Redfield equation seems to behave better under 300 K than under 77 K, which is counter-intuitive (regarding the estimator in Eq. 64).

More results with the relaxation time $\tau_c = 166$ fs (a more challenging case) can be found in Ref. [11].

References

[1] Seogjoo J. Jang. 5 - quantum dynamics of molecular excitons. In Seogjoo J. Jang, editor, *Dynamics of Molecular Excitons*, Nanophotonics, pages 107–147. Elsevier, 2020.

[2] Fumiaki Shibata and Toshihico Arimitsu. Expansion formulas in nonequilibrium statistical mechanics. *Journal of the Physical Society of Japan*, 49(3):891–897, 1980.

[3] Lyran Kidon, Eli Y. Wilner, and Eran Rabani. Exact calculation of the time convolutionless master equation generator: Application to the nonequilibrium resonant level model. *The Journal of Chemical Physics*, 143(23):234110, 12 2015.

[4] Lyran Kidon, Haobin Wang, Michael Thoss, and Eran Rabani. On the memory kernel and the reduced system propagator. *The Journal of Chemical Physics*, 149(10):104105, 09 2018.

[5] F. Bloch. Generalized theory of relaxation. *Phys. Rev.*, 105:1206–1222, Feb 1957.

[6] A.G. Redfield. The theory of relaxation processes. In John S. Waugh, editor, *Advances in Magnetic Resonance*, volume 1 of *Advances in Magnetic and Optical Resonance*, pages 1–32. Academic Press, 1965.

[7] Abraham Nitzan. *Chemical Dynamics in Condensed Phases: Relaxation, Transfer and Reactions in Condensed Molecular Systems*. Oxford University Press, 2006.

[8] A.O Caldeira and A.J Leggett. Quantum tunnelling in a dissipative system. *Annals of Physics*, 149(2):374–456, 1983.

[9] H P Breuer and F Petruccione. *The Theory of Open Quantum Systems*. Oxford University Press, 2002.

[10] Francesco Campaioli, Jared H. Cole, and Harini Hapuarachchi. Quantum master equations: Tips and tricks for quantum optics, quantum computing, and beyond. *PRX Quantum*, 5:020202, Jun 2024.

[11] Andrés Montoya-Castillo, Timothy C. Berkelbach, and David R. Reichman. Extending the applicability of Redfield theories into highly non-Markovian regimes. *The Journal of Chemical Physics*, 143(19):194108, 11 2015.

[12] RE Fenna and BW Matthews. Chlorophyll arrangement in a bacteriochlorophyll protein from Chlorobium limicola. *Nature*, 258:573–577, 1975.

[13] Yi-Fen Li, Wenli Zhou, Robert E. Blankenship, and James P. Allen. Crystal structure of the bacteriochlorophyll a protein from chlorobium tepidum11edited by r. huber. *Journal of Molecular Biology*, 271(3):456–471, 1997.

[14] Akihito Ishizaki and Graham R. Fleming. Theoretical examination of quantum coherence in a photosynthetic system at physiological temperature. *Proceedings of the National Academy of Sciences*, 106(41):17255–17260, 2009.

[15] Jing Zhu, Sabre Kais, Patrick Rebentrost, and Alán Aspuru-Guzik. Modified scaled hierarchical equation of motion approach for the study of quantum coherence in photosynthetic complexes. *The Journal of Physical Chemistry B*, 115(6):1531–1537, 2011.

[16] Xin He and Jian Liu. A new perspective for nonadiabatic dynamics with phase space mapping models. *The Journal of Chemical Physics*, 151(2):024105, 07 2019.

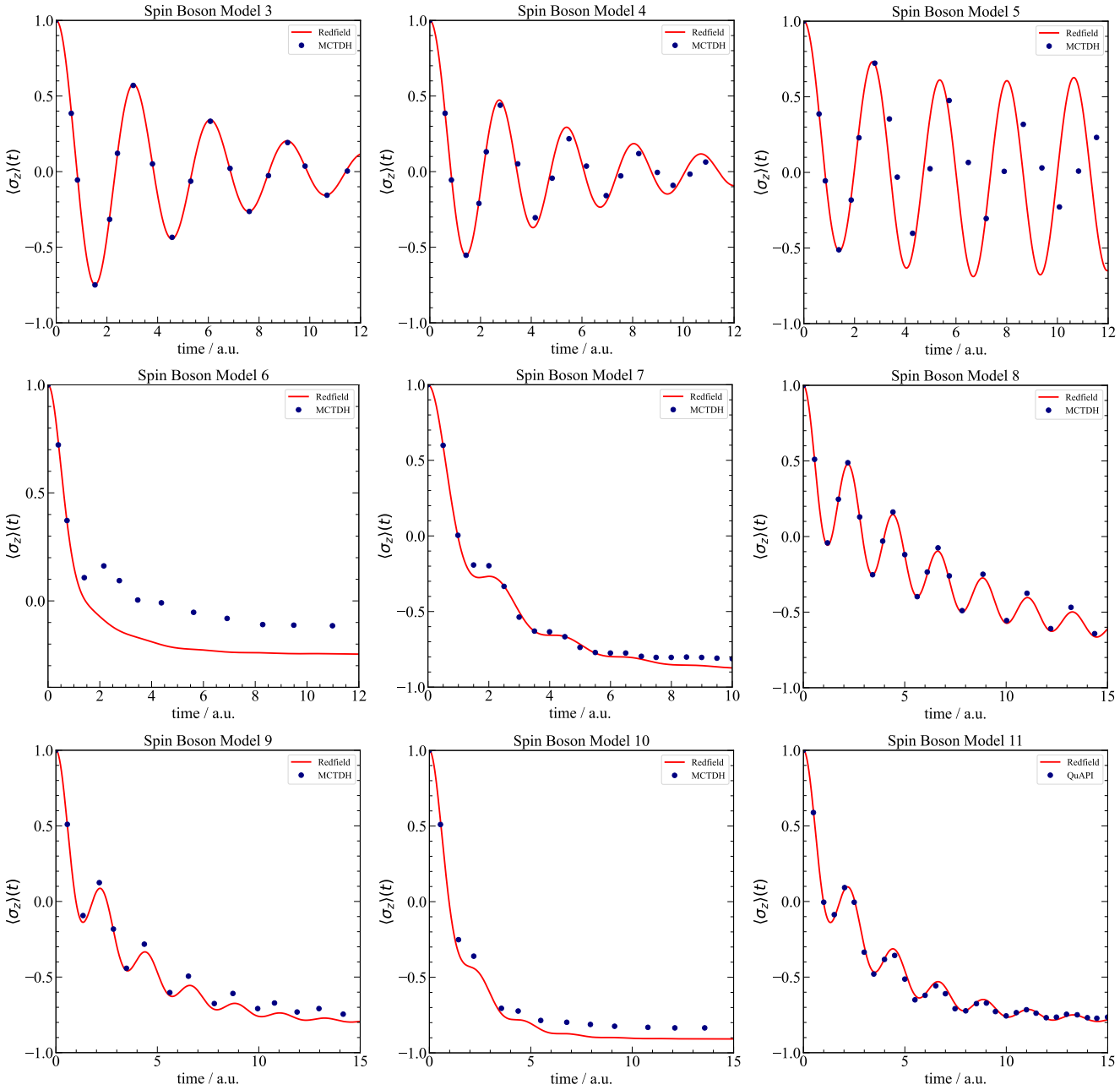

Figure 1: Numerical results of the spin-boson model with Ohmic spectral density. The models are taken from Ref. [16] with orginal labeling. Results are compared with the numerically exact MCTDH or QuAPI. The model parameters are as follows.

(a) Model 3: $\epsilon = 0,\ \Delta = 1,\ \beta = 0.25,\ \omega_c = 5,\ \alpha = 0.02$;
(b) Model 4: $\epsilon = 0,\ \Delta = 1,\ \beta = 0.25,\ \omega_c = 1,\ \alpha = 0.1$;
(c) Model 5: $\epsilon = 0,\ \Delta = 1,\ \beta = 0.25,\ \omega_c = 0.25,\ \alpha = 0.4$;
(d) Model 6: $\epsilon = 1,\ \Delta = 1,\ \beta = 0.25,\ \omega_c = 1,\ \alpha = 0.4$;
(e) Model 7: $\epsilon = 1,\ \Delta = 1,\ \beta = 5,\ \omega_c = 2,\ \alpha = 0.4$;
(f) Model 8: $\epsilon = 1,\ \Delta = 1,\ \beta = 5,\ \omega_c = 2.5,\ \alpha = 0.1$;
(g) Model 9: $\epsilon = 1,\ \Delta = 1,\ \beta = 5,\ \omega_c = 2.5,\ \alpha = 0.2$;
(h) Model 10: $\epsilon = 1,\ \Delta = 1,\ \beta = 5,\ \omega_c = 2.5,\ \alpha = 0.4$;
(i) Model 11: $\epsilon = 1,\ \Delta = 1,\ \beta = 10,\ \omega_c = 2.5,\ \alpha = 0.2$.

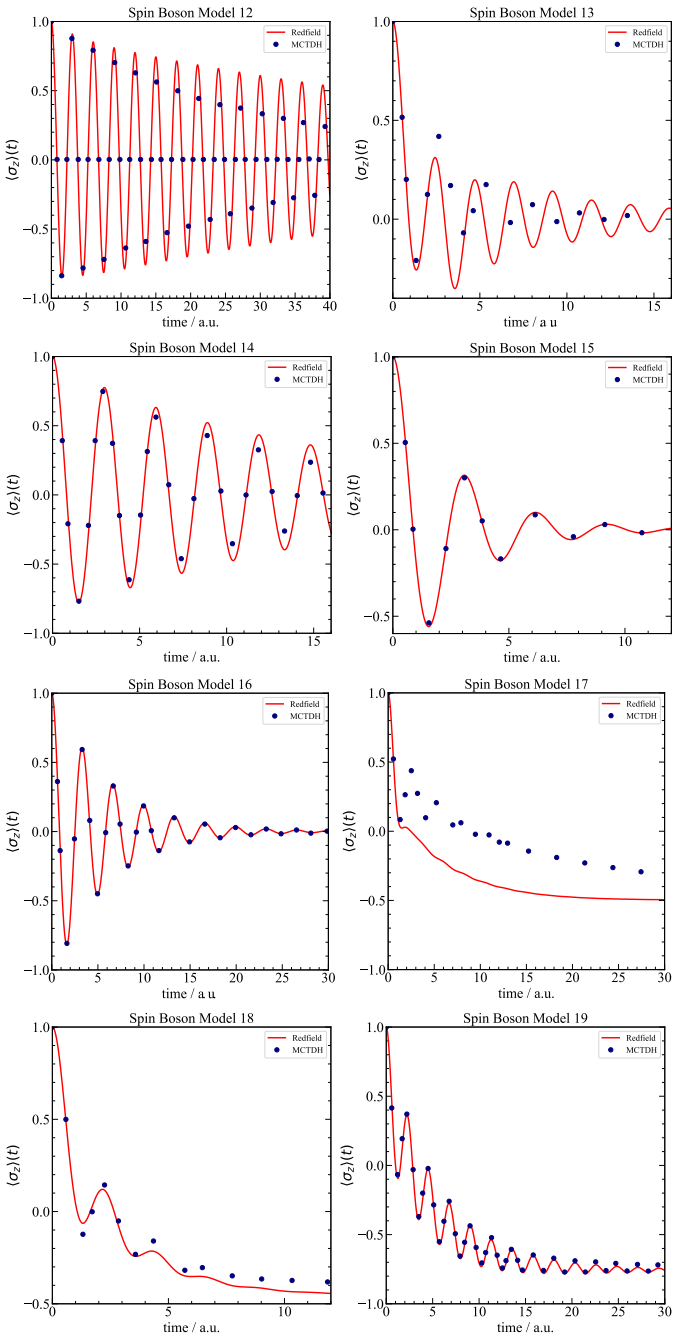

Figure 2: Numerical results of the spin-boson model with Debye spectral density. The models are taken from Ref. [16] with orginal labeling. Results are compared with the numerically exact MCTDH. The model parameters are as follows.

(a) Model 12: $\epsilon = 0,\ \Delta = 1,\ \beta = 0.5,\ \omega_c = 0.25,\ \lambda = 0.025$;
(b) Model 13: $\epsilon = 0,\ \Delta = 1,\ \beta = 0.5,\ \omega_c = 0.25,\ \lambda = 0.25$;
(c) Model 14: $\epsilon = 0,\ \Delta = 1,\ \beta = 5,\ \omega_c = 0.25,\ \lambda = 0.25$;
(d) Model 15: $\epsilon = 0,\ \Delta = 1,\ \beta = 0.5,\ \omega_c = 5,\ \lambda = 0.25$;
(e) Model 16: $\epsilon = 0,\ \Delta = 1,\ \beta = 50,\ \omega_c = 5,\ \lambda = 0.25$;
(f) Model 17: $\epsilon = 1,\ \Delta = 1,\ \beta = 0.5,\ \omega_c = 0.25,\ \lambda = 0.25$;
(g) Model 18: $\epsilon = 1,\ \Delta = 1,\ \beta = 0.5,\ \omega_c = 5,\ \lambda = 0.25$;
(h) Model 19: $\epsilon = 1,\ \Delta = 1,\ \beta = 50,\ \omega_c = 5,\ \lambda = 0.25$.

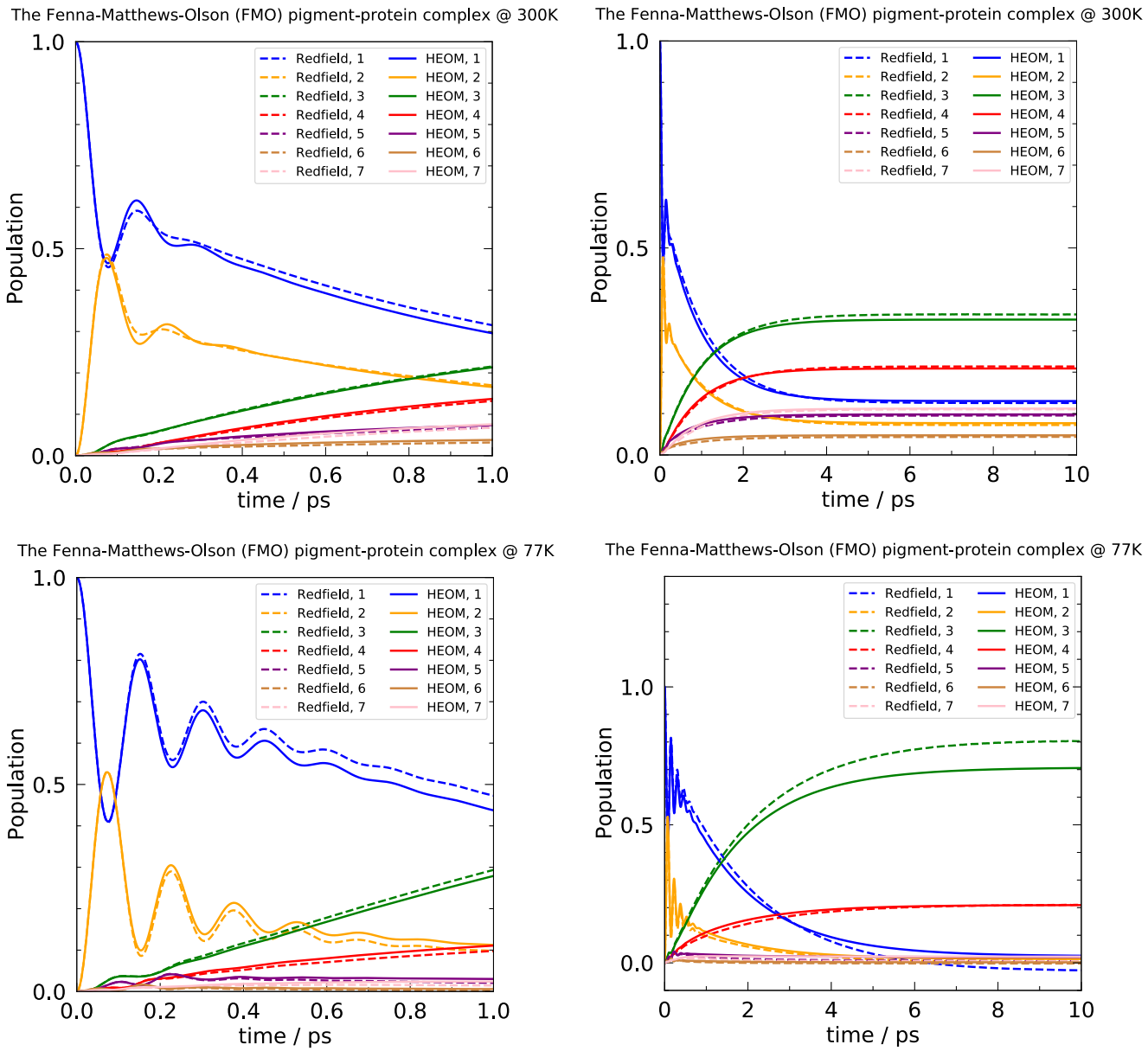

Figure 3: Numerical results of the FMO model under 300 K and 77 K, respectively. The short time (1 ps) and long time (10 ps) dynamics are presented. The Redfield results (dashed lines) are compared with the numerically exact HEOM results (solid lines).